8924 *Macromolecules* **2010**, *43*, 8924–8932
DOI: 10.1021/ma100265f

Macromolecules
ARTICLE

Miniemulsion Polymerization of 2-Ethylhexyl Acrylate. Polymer Architecture Control and Adhesion Properties

Amaia Agirre,[†] Julia Nase,[‡] Elise Degrandi,[‡] Costantino Creton,[‡] and José M. Asua*[,†]

[†]*Institute of Polymer Materials (POLYMAT) and Grupo de Ingeniería Química, Edificio Korta I+D+I University of the Basque Country, 20018 Donostia-San Sebastián, Spain, and* [‡]*Laboratoire de Physico-Chimie des Polymères et des Milieux Dispersés ESPCI 10, rue Vauquelin 75231 Paris Cedex 05, France*

Received February 3, 2010; Revised Manuscript Received September 15, 2010

ABSTRACT: The feasibility of independent control of the gel fraction and sol molecular weight distribution in the miniemulsion polymerization of 2-ethylhexyl acrylate using symmetrical and nonsymmetrical cross-linkers and a chain transfer agent was investigated. It was found that the very reactive symmetrical cross-linker had only a limited effect on polymer architecture, whereas the nonsymmetrical cross-linker and the chain transfer agent had a profound effect allowing decoupling gel and sol molecular weight. Adhesive properties were mainly controlled by the gel content of the polymer.

Introduction

Pressure-sensitive adhesives (PSA) are viscoelastic materials that can adhere strongly to solid surfaces upon application of light contact pressure and short contact time.[1−13] PSAs are commonly applied as a polymeric thin layer over a substrate and can be a part of products ranging from simple applications (e.g., self-adhesive envelopes and self-adhesives stamps) to highly sophisticated ones (automotive, aerospace, and electronic industries).

Among different base polymers used in making PSAs, acrylates (poly(butyl acrylate), poly(2-ethylhexyl acrylate)) have enjoyed the fastest growth in commercial applications. Their popularity is due to optical clarity, UV light and oxidation stability, low toxicity, and relative low cost.[7,9]

The application of these products is mainly dominated by the polymer properties, which in turn depend on the T_g and on the polymer architecture. The T_g is easily controlled by varying the relative amounts of the soft and hard comonomers. However, the independent control of the sol molecular weight distribution (MWD) and the gel fraction is challenging. In the polymerization of neat acrylic monomers, because of their peculiar polymerization mechanism, sol molecular weight and gel fraction are correlated.[14,15] The higher the gel fraction the lower the sol molecular weight.[14,15] Gel fraction can be easily reduced by using chain transfer agents (CTA), but the sol MWD remains essentially unaffected.[16] Chauvet et al.[17] showed that, in the emulsion polymerization of butyl acrylate, it is possible to achieve a certain degree of independent control of the sol molecular weight and the gel fraction by simultaneously using a CTA and allyl methacrylate (AMA) as cross-linker.

High-performance PSAs are based on 2-ethylhexyl acrylate (2EHA). This monomer has a glass transition temperature ($T_g = -85$ °C) lower than butyl acrylate ($T_g = -54$ °C) and is more prone to suffer chain transfer to polymer, which yields a different network structure.[15,18] The combination of these characteristics leads to improved adhesion properties. However, 2-EHA is also affected by the correlation between sol molecular weight and gel fraction.[15] Therefore, decoupling of gel content and sol molecular weight would extend the range of properties of these PSAs.

The objectives of this work are twofold. First, to investigate the feasibility of independent control of gel fraction and sol molecular weight in the miniemulsion polymerization of 2-ethylhexyl acrylate using symmetrical and nonsymmetrical cross-linkers and a CTA (*n*-dodecyl mercaptan). Miniemulsion polymerization was used to avoid the diffusional limitations associated with the use of a very low water solubility monomer and a chain transfer agent in emulsion polymerization.[19,20] The symmetrical cross-linker was ethylene glycol dimethacrylate (EGDMA), which has very reactive functional groups. The nonsymmetrical cross-linker was allyl methacrylate, which has two reactive groups of very different reactivity. The methacrylic group is more reactive than the acrylates, and the allyl group is very unreactive. Second, to study the effect of the polymer architecture on the adhesive properties (tack, peel strength, and shear resistance).

Experimental Section

Materials. 2-Ethylhexyl acrylate (2-EHA) (Quimidroga), methacrylic acid (MAA) (Aldrich), and stearyl acrylate (SA) (Aldrich) were used as received. Dowfax 2A-1 ((alkyldiphenyloxide disulfonate, Dow Chemical Company) was used as emulsifier, and hexadecane (Sigma-Aldrich) was used as costabilizer. Ammonium persulfate (Fluka Chemika) was used as initiator. Ethylene glycol dimethacrylate (EGDMA) (Fluka) and allyl methacrylate (AMA) (Aldrich) were used as cross-linkers, whereas *n*-dodecyl mercaptan (Merck) was used as a chain transfer agent (CTA). THF (99.9% GPC grade, Scharlab) was used as a solvent for the Soxhlet extractions and the sol molecular weight measurements.

Preparation of the Miniemulsions. The miniemulsions were prepared as follows. Dowfax 2 A-1 was dissolved in water to prepare the aqueous phase, and all the monomers, the cross-linker, and the chain transfer agent were mixed to prepare the oil phase. In order to minimize the Ostwald ripening effect, a costabilizer is needed.[20] A costabilizer is a low molecular weight highly water-insoluble compound. Hexadecane is frequently used as costabilizer,[21] but it is unreactive and hence it increases the volatile organic compound (VOC) content of the final latex. In this work, a highly water-insoluble monomer (stearyl acrylate) was used to minimize the Ostwald ripening effect. As it is incorporated into the polymer, it does not increase the VOC content of the latex. The oil phase was added to the aqueous

---

*Corresponding author. E-mail: jm.asua@ehu.es.

Table 1. Formulations Used To Prepare the Seeds

ingredient	amount (g)
water	719.22
2-ethylhexyl acrylate	671.19
methacrylic acid	13.66
stearyl acrylate/hexadecane[a]	27.96
Dowfax 2A-1	15.21
$(NH_4)_2S_2O_8$	3.43

[a] Used in seed 2.

Table 2. Latexes Synthesized Varying the Concentration of CTA and Cross-Linker[a]

latex	CTA (mol %)	X-linker (mol %)
1	0	0
2	2.96×10^{-3}	0
3	2.96×10^{-3}	0
4	0	1.16×10^{-3}
5	0	1.82×10^{-3}
6	0	1.82×10^{-3} *
7	2.47×10^{-4}	1.16×10^{-3}
8	7.41×10^{-4}	1.16×10^{-3}
9	1.48×10^{-3}	6.56×10^{-4}
10	0	2.4×10^{-3} *

[a] EGDMA; (*) AMA.

Table 3. Formulations Used in the Seeded Semicontinuous Miniemulsion Polymerizations[a]

ingredient	initial charge (g)	stream 1 (g)	stream 2 (g)
seed	100/70*		
water		241.06/169.2*	18.87/15.42*
2-ethylhexyl acrylate		236.16/165.9*	
methacrylic acid		4.82/3.4*	
stearyl acrylate		9.68/6.85*	
N-dodecyl mercaptan		0−1.48/0*	
EGDMA		0−0.56/0.61*	
AMA		0−0.73/0*	
Dowfax 2 A-1		5.38/3.76*	
$(NH_4)_2S_2O_8$			1.13/0.88*

[a] (*) Formulation employed in run 5.

phase and mixed for 20 min with a magnetic stirrer at 700 rpm. This coarse emulsion was miniemulsified in a two-valve high-pressure homogenizer (Manton Gaulin homogenizer, $P_1 = 4000$ bar, $P_2 = 400$ bar, for 7 cycles). The solids content of the miniemulsion was about 50 wt %. To prevent overheating during miniemulsification, the homogenizer had a refrigerating system.

Miniemulsion Polymerizations. Seeded miniemulsion polymerizations were carried out. The seed poly(2EHA-*co*-MAA) was prepared batchwise using the formulation shown in Table 1 in a 750 mL glass jacketed reactor fitted with a reflux condenser, a sampling device, a N_2 inlet, and a stainless steel impeller rotating at 200 rpm. The reaction was carried out at 70 °C for 2 h and kept overnight at 90 °C to decompose the unreacted initiator.

The seeded semicontinuous miniemulsion polymerizations were carried out in a 750 mL glass jacketed reactor fitted with a reflux condenser, a sampling device, a N_2 inlet, two feeding inlets, and a stainless steel anchor stirred equipped with two blade impellers rotating at 200 rpm.

Table 2 summarizes the latexes synthesized, and Table 3 details the formulations used. Latex 1 was synthesized without neither CTA nor cross-linker and was used as a reference. The effect of using CTA was studied in runs 2 and 3. In both cases, the same total amount of CTA was used, but in run 2, the CTA was fed along the whole feeding period, whereas in run 3, all the CTA was fed during the last 30 min of the feeding period. The effect of the cross-linker concentration was studied in runs 4 and 5. In order to study the effect of the reactivity of the functional groups of the cross-linker, runs 6 and 10 were carried out using allyl methacrylate. The simultaneous use of cross-linker and CTA was studied in runs 7−9.

The miniemulsion polymerizations were carried out as follows: 100 g of seed 1 (dp = 169 nm, about 70% gel content and 50% solids content) was charged into the reactor and heated until it reached 70 °C. Then, the monomer miniemulsion containing the CTA and cross-linker (when used) and an aqueous solution of initiator were fed in separate streams for 3 h. Upon finishing the addition, the reaction was kept batchwise for 60 min. Because we run out of seed, another seed (seed 2: dp = 219 nm about 42.5% gel content and 50% solids content) was prepared and used in run 3. The differences in the size were due to the different costabilizer used (stearyl acrylate vs hexadecane). This affected the kinetics and hence the final conversion achieved (99.2% for seed 1 vs 100% for seed 2). In addition, in acrylic systems, the gel formation is the result of intermolecular chain transfer to polymer and termination by combination which takes place mainly when the ratio between monomer and polymer is low. Therefore, most of the gel is formed in the final stages of the batch polymerization and small differences in final conversion (99.2% for seed 1 vs 100% for seed 2) results in substantial changes in gel content (70% for seed 1 vs 42.5% for seed 2).

Characterization. Monomer conversion was determined by gravimetry. The instantaneous conversion, X_i, was defined as the amount of polymer in the reactor divided by the total amount of monomer and polymer in the reactor. The overall conversion was the amount of polymer in the reactor divided by the amount of monomer plus the amount of polymer in the formulation.

Particle size was measured by dynamic light scattering (DLS) using a Zetasizer Nano Z (Malvern Instruments). Particle size distribution was determined by capillary hydrodynamic fractionation (CHDF, Matec Applied Sciences, model 2000). The equipment was operated at 35 °C using a flow rate of 1.4 mL/min of carrier fluid (1/4X, from Matec), and the detector wavelength was set to 200 nm.The sample concentration employed was less than 0.5 wt %.

The number of particles (N_p) was calculated from the particle size measured by DLS and the instantaneous conversion determined by gravimetry. New droplets may affect the particle size, but the effect is expected to be weak because the fraction of monomer droplets should be low at the high conversions achieved in the polymerization.

The gel fraction and the swelling degree were determined by Soxhlet extraction. The process consisted in a 24 h continuous extraction with THF under reflux. After the extraction, the samples were dried and the gel content was calculated as the ratio between the weight of the polymer that was not extracted and the initial amount of polymer. This method provides accurate results for gel contents above about 20%. Lower gel contents are not accurately measured. The swelling degree was calculated as the ratio between the weight of the swollen gel after 24 h extraction and the weight of the dry gel.

The sol molecular weight was determined by size exclusion chromatography (SEC, Waters). The setting consists in a pump, a differential refractometer (Waters 2410), and three columns in series (Styragel HR2, HR4, and HR6; with pore sizes from 10^2 to 10^6 Å). The analyses were performed at 35 °C, and THF was used as solvent at a flow rate of 1 mL/min. The solution of sol polymer in THF recovered from the Soxhlet extraction was dried in a ventilated oven. The dried polymer was redissolved in THF. Afterward, it was filtered (polyamide filter $\Phi = 0.45\,\mu$m), and the sample was injected into the SEC.

Adhesion Properties. The adhesive performance of the PSAs produced (tack, peel strength, and resistance to shear) was evaluated. Tack was determined by using an instrumented probe tack technique.[22,23] 100 μm thick films were cast from the latexes on a standard microscope glass slide by water evaporation at room temperature until constant weight was achieved. The sample was fixed on the upper plate of the probe tack apparatus, whereas the probe (6 mm diameter polished stainless steel) was fixed on the mobile lower shaft and connected to the load cell.

The tack test procedure consisted of first bringing the probe into contact with the film at a constant speed of 20 μm/s. Then, a compressive force of 5 N was applied. The probe was left in contact with the adhesive for 1, 10, or 100 s. Finally, the probe was removed at a constant speed, which was varied from 1, 10, to 100 μm/s. The entire process of contact between the probe and the film and the subsequent debonding were followed by a video camera on a microscope. The force needed to detach the adhesive from the probe and the deformation provoked during the debonding process were recorded. All experiments were carried out at room temperature.

Peel resistance was determined by means of the T-peel test[24] over polypropylene (PP) at room temperature. In these tests, a tape (4 cm × 2.5 cm) was applied to a polypropylene substrate, and the free end was clamped to the upper jaw of an Instron tensile tester, which pulled the tape at a constant speed of 300 mm/min. The average force required to peel away the tape was recorded.

Shear resistance was assessed by the holding power shear test.[25,26] This test consisted in applying a standard area of tape (2.5 cm × 2.5 cm) on a panel holding 1 kg until failure. The experiments were performed at 30 °C. The adhesive films used in the tests were obtained under standard conditions ($T = 23$ °C and humidity = 55%) by spreading the latex over a flame-treated 29 μm thick polypropylene using a multiple gap applicator with reservoir. The gap employed was of 120 μm. A 1 wt % solution of a superspreader (Silwet L-77) was previously added to the latex to improve wetting and consequently film quality. The films were dried at room temperature for 20 min. Afterward, they were placed in a well-ventilated oven at 60 °C for 10 min to evaporate completely the water and finally were allowed to cool down at room temperature for 10 min before being cut to the desired dimensions for each test.

The mechanical properties corresponding to the nonlinear elastic properties were measured in a tensile testing machine (Instron 5565). The tested samples were rectangular: 1 mm thick, 4 mm wide, and 15 mm long (length between clamps). They were prepared at the desired thickness by casting the latex in silicone molds at room temperature. All the tests were performed at room temperature and at two different crosshead speeds, 1.5 and 15 mm/s corresponding to an initial strain rate of 0.1 and 1 s^{-1}, respectively.

Small-amplitude oscillatory measurements in the linear regime were carried out in plate–plate mode (diameter 12 mm) in a stress-controlled TA Instrument AR-G2 rheometer. The samples tested were circular 1 mm thick and 12 mm diameter. They were prepared at the desired thickness by casting the latex in silicone molds (T = 23 °C; humidity = 55%).

Results and Discussion

Effect of Process Conditions on Polymer Architecture. Figure 1 presents the kinetics of the reactions carried. It can be seen that most of the processes occurred under starved conditions and that neither the CTA concentration nor the concentration of cross-linker affected significantly the polymerization rate. The lower instantaneous conversion achieved in runs 6 and 10 might be due to low reactivity of the allyl group of AMA. In addition, in run 3, about 100 g of miniemulsion was rapidly added at the beginning of the process because of an error in the feeding system.

Figure 2 presents the particle size distribution of the latexes as measured by CHDF. With the exception of latex 3, all latexes presented a similar PSD: a main peak around 200 nm with small shoulders at the small (< 100 nm) and large (> 300 nm) ends of the distribution. The diameter of the miniemulsion droplets fed was in the range of 168–200 nm (Table 4). No explanation for the different PSD of latex 3 can be offered. Figure 3 shows that the average particle size measured by DLS was not affected by the CTA and cross-linker concentrations. It remained constant for most of the process, indicating a continuous nucleation, which led to a continuous increase of number of polymer particles (Figure 4). However, it can be seen (Figure 3) that the particle size increased for the first 40 min and then remained more or less constant. At any time during the process a fraction of the monomer of the newly fed droplets diffused to the existing particles. The effect of this monomer on the size of the existing particles depends on both the size of the particles (the smaller the size, the larger the effect on the diameter caused by a given amount of monomer) and the number of particles (the smaller the number, the larger the increase in size because each

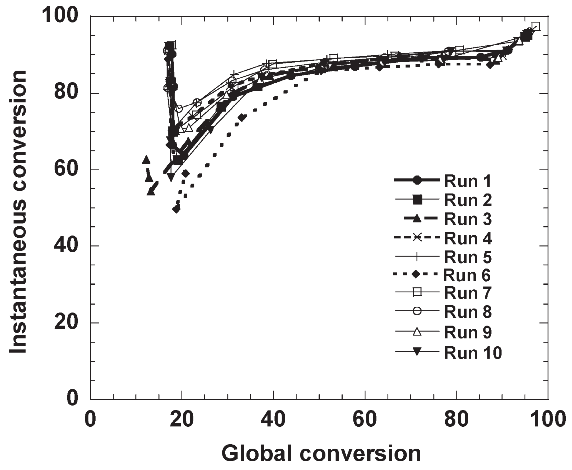

Figure 1. Evolution of the instantaneous conversion during the synthesis of the latexes 1–10.

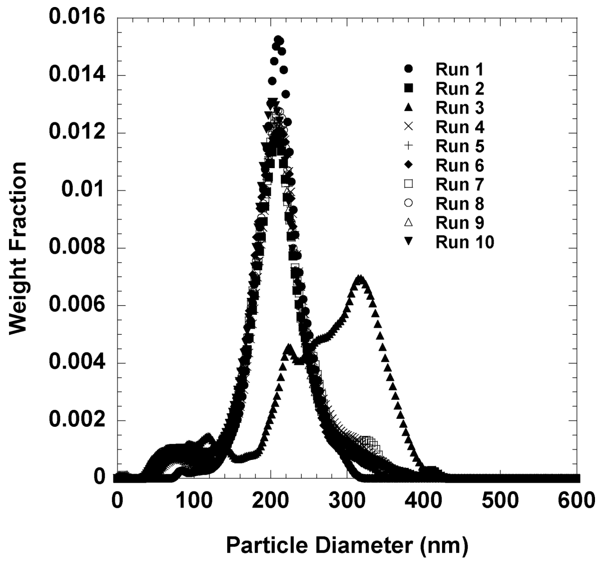

Figure 2. Particle size distribution of the final latexes.

Table 4. Droplet Size of the Miniemulsions Fed in the Semicontinuous Polymerization

run	D_d (nm)	run	D_d (nm)
1	168	6	163
2	172	7	n.a.
3	177	8	172
4	183	9	165
5	200	10	177

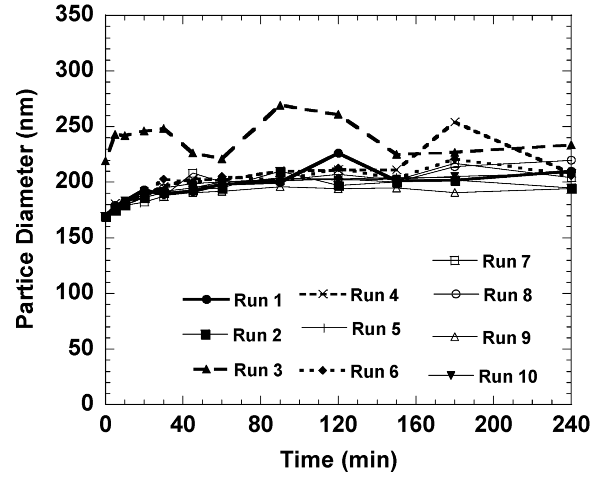

Figure 3. Evolution of the average particle size during the synthesis of latexes 1−10.

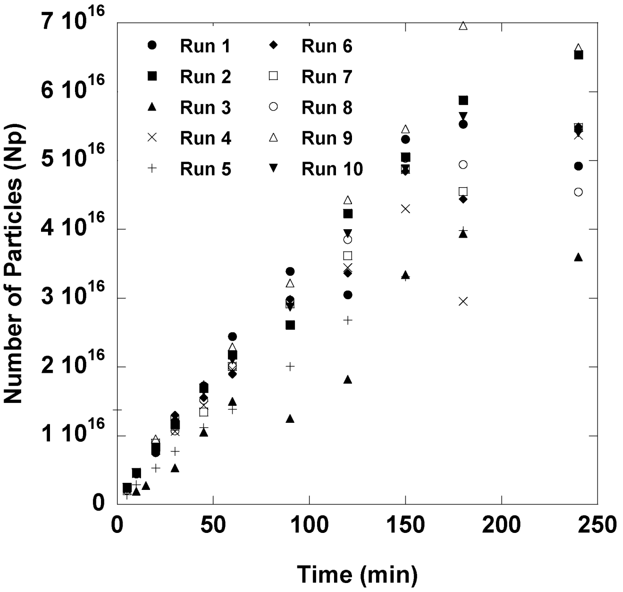

Figure 4. Evolution of the average number of polymer particles during the synthesis of latexes 1−10.

particle receives a larger amount of monomer). Therefore, the effect was larger at the beginning of the process when the latex was formed by less and smaller particles. In addition, new particles were continuously formed, and this counteracted the effect of the growth of the existing particles and the average particle size measured by DLS. On the other hand, the fact that the average size of the polymer particles was similar to that of the droplets suggests that droplet nucleation was the main nucleation mechanism. The small fraction of particles smaller than 100 nm (Figure 2) might be due to homogeneous nucleation. Although nucleation continuously occurred during the process, only a fraction of the entering droplets was nucleated (Figure 5). The probability of radical entry in monomer droplets decreases with the number of polymer particles present in the system. This means that in a semicontinuous polymerization using miniemulsion feeding the probability of nucleation of the droplets entering into the reactor decreases along the process.[27] From Figures 1−5 it can be concluded that neither the CTA nor the cross-linker affected the kinetics of polymerization.

Figures 6 and 7 present the effect of the CTA concentration on gel content and sol MWD. It can be seen that when the CTA was fed with the monomers during the whole process (run 2), no gel was formed. However, when the same amount of CTA was fed in the last 30 min of the process (run 3), the gel fraction was lower than in the absence of CTA (run 1) but still substantial. The increase in swelling when the gel fraction decreased indicates that the cross-linking density increased as the gel fraction increased. On the other hand, the sol molecular weight decreased when the CTA was fed during the whole process. In this case the effect was stronger than for butyl acrylate,[16] and the effect of the CTA on the kinetic chain length was not compensated by the fraction of chains that was not incorporated into the gel, likely because of the stronger intermolecular chain transfer to polymer of the 2EHA. The addition of the CTA at the end of the process resulted in a broader MWD of the sol fraction. There were two reasons for this result. On one hand, the tail of low molecular weight was the result of the high concentration of CTA at the end of the process, which led to a severe reduction of the kinetic chain length. The high molecular weight tail consisted of polymer chains formed before starting the addition of CTA that were not incorporated into the gel because in the presence of CTA the kinetic chain length of the branches was relatively short limiting the increase in size of the polymer chains.

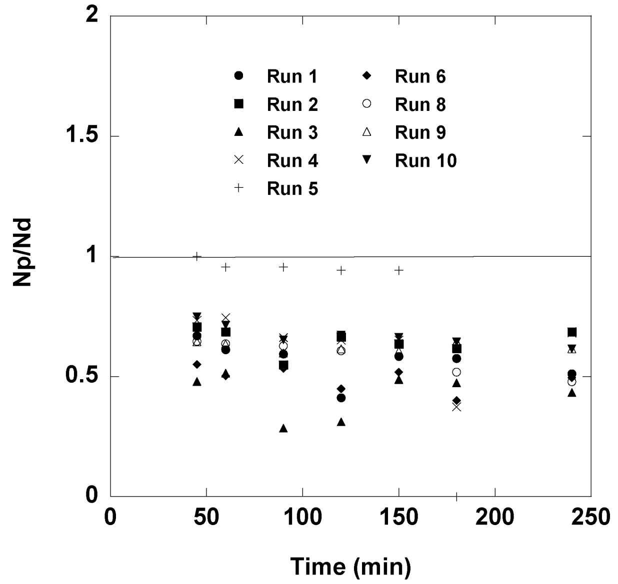

Figure 5. Evolution of the ratio between the number of particles and the number of droplets fed along the reaction.

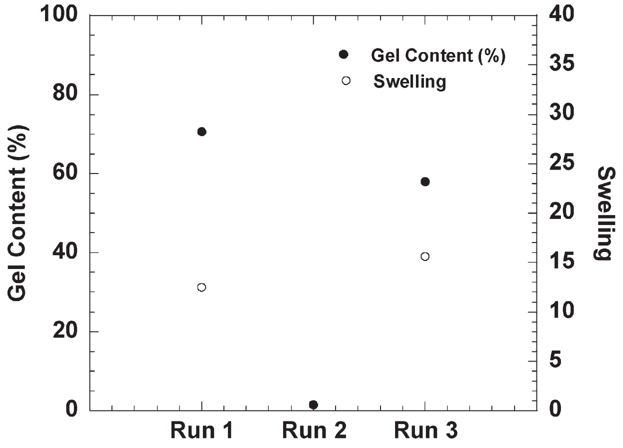

Figure 6. Effect of the CTA concentration on the gel fraction.

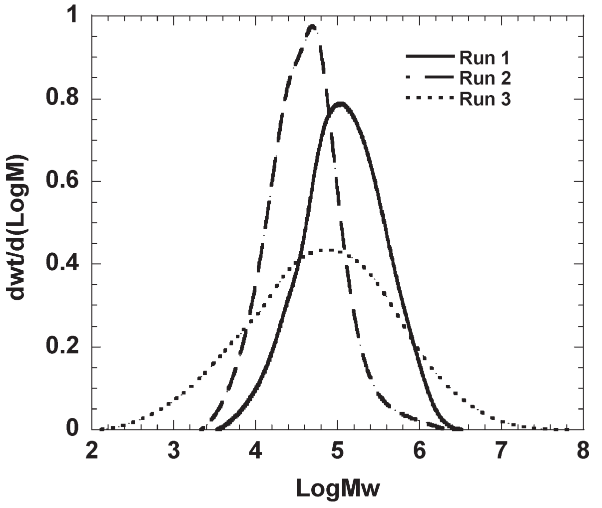

Figure 7. Effect of the CTA concentration on the sol MWD.

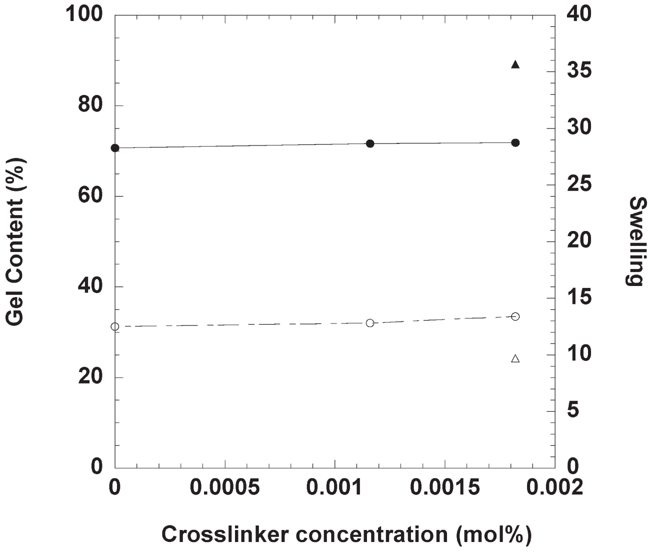

Figure 8. Effect of the concentration of cross-linker on the gel fraction (solid symbols) and swelling (open symbols) (●, EGDMA; ▲, AMA).

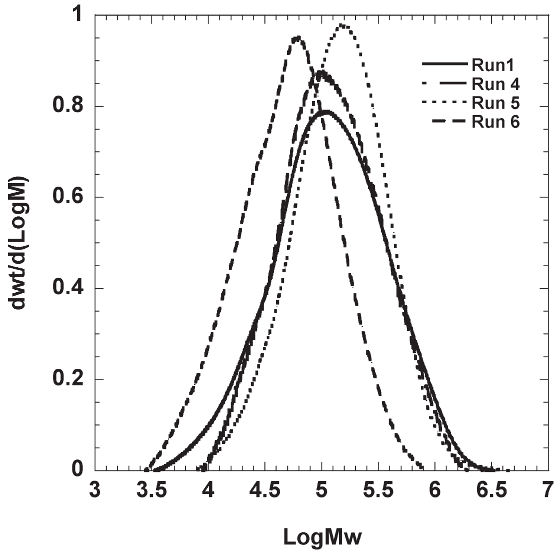

Figure 9. Effect of the concentration of cross-linker on the sol MWD of the final latexes.

Scheme 1. Primary Cyclization

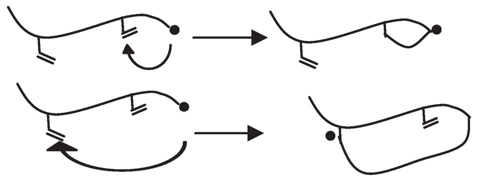

Figures 8 and 9 present the effect of the concentration of cross-linker (EGDMA) on the gel fraction and sol molecular weight distribution. It can be seen that, surprisingly, the cross-linker had almost no effect on either the gel fraction or the sol MWD. Using the swelling degree as a measure of the cross-linking density, Figure 8 shows that the cross-linking density was either constant or slightly increased with the concentration of EDGMA. This may be due to extensive primary cyclization (Scheme 1) which is more pronounced in the case of short cross-linkers.[28−30] Bouvier-Fontes et al.[31] reported that primary cyclization was the cause for which symmetrical highly reactive cross-linkers gave less gel content and cross-linking density than nonsymmetrical ones having one relatively unreactive functional group. Allyl methacrylate is an example of nonsymmetrical cross-linker having functional groups of very different reactivity. Therefore, in order to check this point, the effect of the type of cross-linker, run 6 was carried out with AMA and using the same concentration of cross-linker that in run 5. The gel fraction and the sol MWD are presented in Figures 8 and 9 to facilitate the comparison with the experiments carried out with EGDMA as cross-linker. It can be seen that the use of AMA substantially affected both the gel fraction (which increased) and the sol molecular weight (which decreased because the longer polymer chains were incorporated into the gel fraction). Consistently, the swelling degree was lower than for EGDMA, indicating that the network had a higher cross-linking density.

Figures 10 and 11 show the effect of the CTA concentration on gel fraction and sol MWD in the presence of cross-linker. It can be seen that the gel fraction decreased with the concentration of CTA. Swelling was not measured for latex 8 because the low amount of gel compromised the accuracy of the measurement. The effect of CTA concentration on sol MWD in the presence of cross-linker is interesting because it led to broader MWDs than that obtained using only cross-linker. Both the low and the high molecular weight tails can be explained by the decrease of the kinetic chain length when the concentration of CTA increased. The low molecular weight tail was due to the shorter chains produced in the presence of CTA. The reduction of the kinetic chain length also affected the high molecular weight tail because the branches formed on long polymer chains were shorter limiting the size of the branched chains that did not reach the size needed to become gel, and hence they remained as sol polymer. An additional experiment was carried out (run 9) using a lower concentration of cross-linker and a higher concentration of CTA than in run 8. The gel content was further reduced (about 5%), and the sol MWD shifted to lower values (not shown here).

Effect of Polymer Architecture on Adhesion Performance. It was found that for most of the synthesized latexes the gel fraction was the variable that had the strongest influence on the adhesive properties. Figure 12 presents the effect of the gel fraction on the work of adhesion measured by the probe tack technique at different contact times using probe removal speed of 10 μm/s (Figure 12a) and at a contact time of

10 s and different probe removal speeds (Figure 12b). When adhesive failure occurs, the work of adhesion is the work needed to fully detach the adhesive from the substrate. When cohesive failure occurs, the work of adhesion is the work needed to deform the polymer until fracture. It can be seen that the work of adhesion increased with the gel content until a maximum was reached. For higher gel contents, the work of adhesion decreased. In the set of data available, this maximum is about 15% of gel (corresponding to latex 8), but gel contents between 15% and 50% might present higher values of the work of adhesion. It is worth pointing out that in the samples with gel content up to 15% (latexes 2, 8, and 9) the sol molecular weight increased with the gel content. For these latexes, a cohesive failure was observed, and the increase in the work of adhesion was due to the increase of the cohesion of the adhesive as gel (and perhaps sol molecular weight) increased. For higher gel contents, the work of adhesion decreased with the gel fraction because as shown in Figure 13, the material became too elastic and the stress needed to deform the adhesive exceeded that needed to detach it from the substrate.

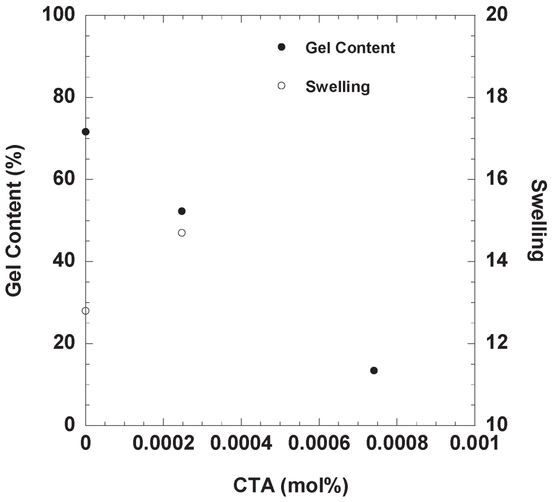

Figure 10. Effect of the concentration of CTA on the gel fraction and swelling of the final latexes synthesized using 1.16 × 10^{-3} mol % of EGDMA.

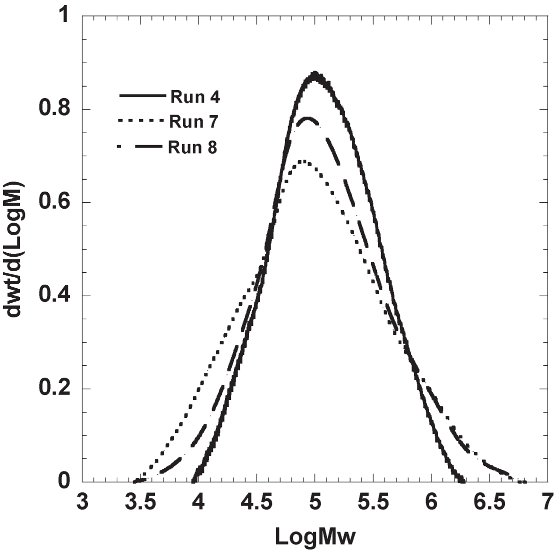

Figure 11. Effect of the concentration of CTA on the sol MWD of the final latexes using 1.16 × 10^{-3} mol % of EGDMA.

Figure 12 shows that there was a significant effect of the contact time on the work of adhesion for intermediate gel contents, but it was negligible for polymers with low (< 15%) and high (> 80%) gel contents. For the polymers with low gel contents (latexes 2, 8, and 9), the contact time did not affect adhesion because they were liquid-like materials that adhered easily to the substrate in a very short time. The polymers with high gel contents behaved like an elastic material, and hence the contact time used probably did not vary substantially the real contact area with the substrate. On the other hand, and as usually observed for PSA, the work of adhesion increased as the probe release speed increased.

The work of adhesion measured in the probe tack experiment is the result of the interplay between bulk deformation and detachment of the adhesive from the substrate.[32] Actually, most of the work of adhesion is due to the energy needed to deform the bulk of the adhesive before the adhesive detaches from the substrate. As the energy needed to deform a viscoelastic material increases with the strain rate, the work of adhesion increases with the probe release speed.

The behavior of latex 1 is interesting as the work of adhesion obtained with this latex did not fit within the trend observed for the rest of latexes. Latex 1 had a gel content (70%) which was very similar to latex 4 (72%), and both latexes presented similar equilibrium swelling levels (Figure 7) and sol molecular weight distributions (Figure 9). However, latex 1 had a higher work of adhesion on steel surfaces than latex 4, the difference being more pronounced at high contact times and low debonding speeds. Latex 1 was synthesized without cross-linker, whereas latex 4 was prepared with

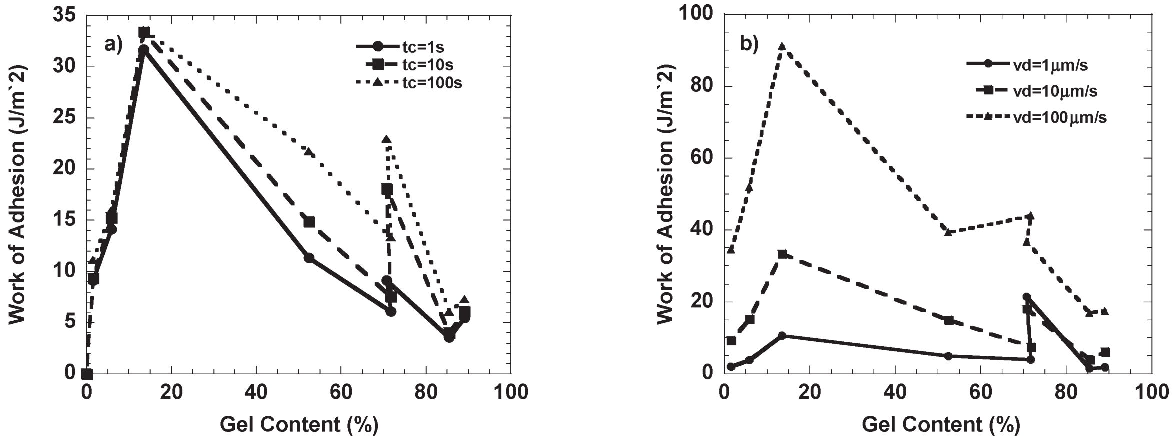

Figure 12. Effect of the gel content on the work of adhesion obtained by the probe test technique at a debonding speed of 10 μm/s and at different contact times (a) and at a contact time of 10 s but different debonding speeds (b).

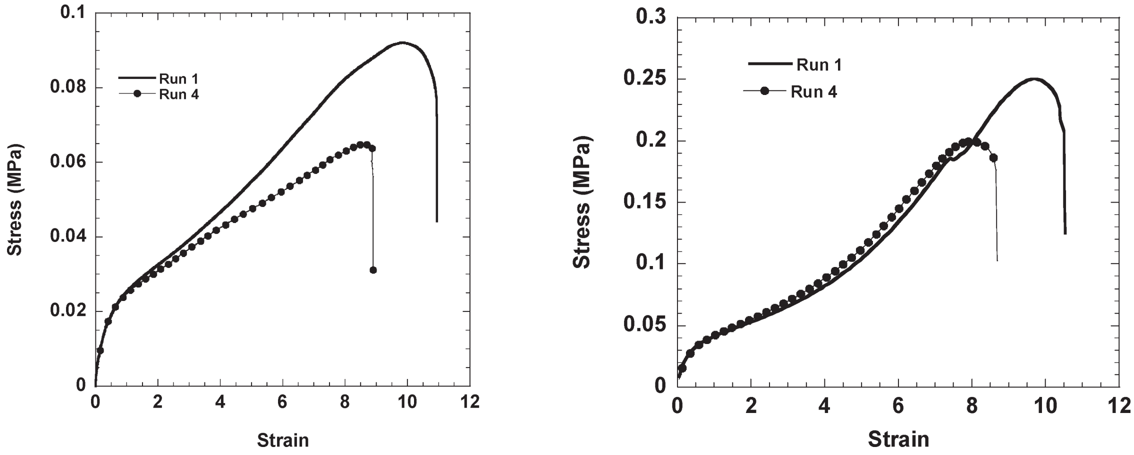

Figure 13. Effect of the gel content on the tensile strength obtained at different speeds: 1.5 mm/s (left) and 15 mm/s (right).

EGDMA. This should result in some differences in the polymer architecture that were not evident in the gel, swelling, and sol MWD.

Because most of the work of adhesion is due to the energy needed to deform the bulk of the adhesive, and the rheological measurements are often very sensitive to differences in polymer architecture, tensile tests of films cast from latexes 1 and 4 were carried out in order to investigate if there were differences in bulk deformation between latexes 1 and 4. Figure 13 shows that under the conditions studied both latexes had a similar behavior. Therefore, the different work of adhesion was not due to differences in bulk deformation.

A rapid detachment of the adhesive from the substrate also causes a decrease of the work of adhesion. According to Deplace et al.,[32] the resistance to detachment is proportional to the ratio between the critical energy release rate, G_c (which is the energy needed to propagate the crack between the adhesive and the substrate), and the Young's modulus of the adhesive, E. The critical energy release rate can be approximated by

$$G_c = G_0(1 + k \tan \delta(\omega)) \tag{1}$$

where G_0 is the resistance to crack propagation at vanishingly low crack velocity, k a constant, and $\tan \delta$ the ratio between the loss, $G''(\omega)$, and the elastic modulus, $G'(\omega)$.

Replacing E by the frequency-dependent elastic modulus and considering that $1 \ll k \tan \delta(\omega)$, one gets

$$\frac{G_c}{E} \approx kG_0 \frac{\tan \delta(\omega)}{G'(\omega)} \tag{2}$$

This means that the resistance to detachment increases with $\tan \delta(\omega)/G'(\omega)$, namely, as the viscous modulus to elastic modulus ratio increases. Figure 14 presents the evolution of this ratio with the frequency for the two latexes. The range of frequencies used in these experiments encompassed the average deformation frequency used in the tack probe experiments (marked in Figure 14). The average strain rate seen by the adhesive layer during a probe test was estimated as $2\Pi v_{\mathrm{deb}}/h_0$ where v_{deb} is the velocity of the probe and h_0 the initial thickness of the adhesive film.[32] Figure 14 shows that the resistance to crack propagation was higher for latex 1, which accounted for the higher work of adhesion (Figure 12). The presence of the cycles arising from the cyclization of EGDMA in run 4 might reduce the number of long entangled pendant chains, resulting in a lower loss modulus and as a consequence in a lower resistance to crack propagation.

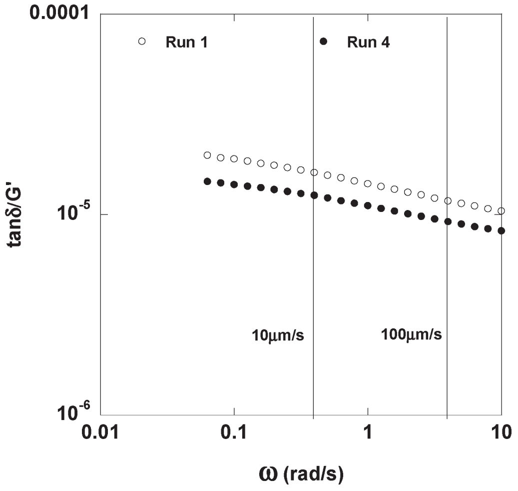

Figure 14. Plot of $\tan \delta/G'$ vs ω of latexes 1 and 4.

Figure 15 shows that the effect of the gel content on the peel resistance was almost the same as the one observed previously for the tack (Figure 8). In both cases, a critical gel content (≈15%) was observed below and above that value peel and tack deteriorated.

In essence, probe tack and peel tests are different techniques to measure the same property—the energy required to debond an adhesive from a determined substrate. This energy depends on the ability of the adhesive to dissipate energy, which in turns depends on the ability of the adhesive to form fibrils on the given substrate. The main difference between both techniques is based on the sample geometry. The peel test which is the main technique employed in the tape industry presents a quite complicated sample geometry which makes the micromechanical analysis of the fibril formation difficult. In contrast, the probe tack technique presents a simple simpler geometry which allows the study of the micromechanical properties of the formation of fibrils during the debonding process.[33,34] However, it should be noted that the contact times are significantly longer and the average strain rates are higher for the peel test samples than for the probe tack samples. Given these differences, the trend is remarkably similar.

Generally speaking, the peel test values and probe test results are rather low while the value of gel content at which the maximum in adhesion is observed is rather low. These results cannot be readily explained by the rheological bulk measurements ($\tan \delta/G'$ values are in the regime where

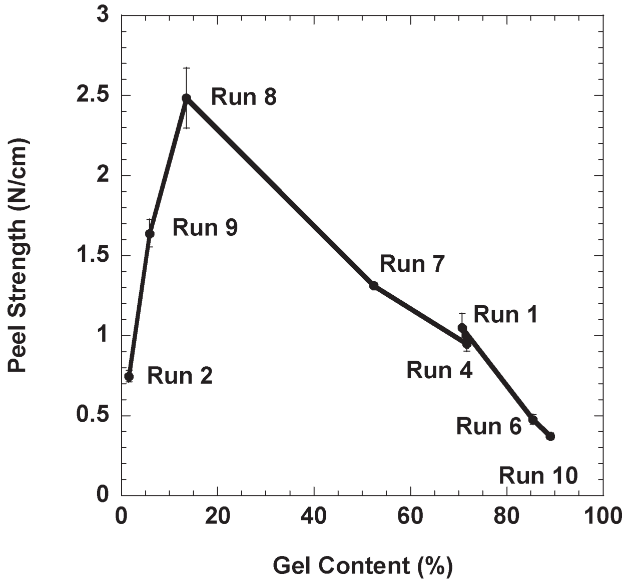

Figure 15. Effect of the gel content on the peel strength obtained by T-peel experiments over polypropylene.

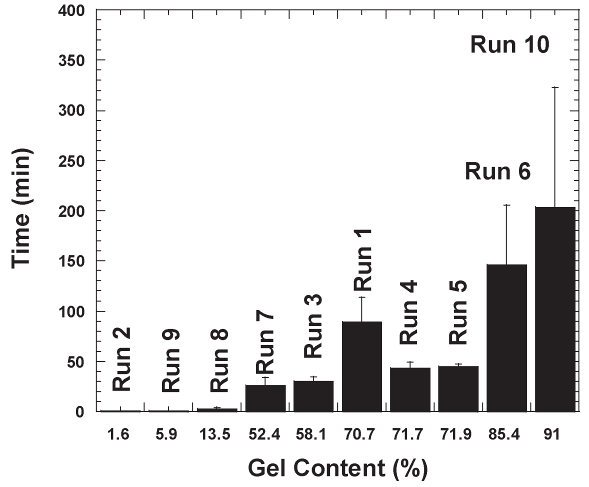

Figure 16. Effect of gel content on the shear resistance measured at 30 °C over polypropylene.

fibrillation should be observed). This suggests that the interfacial interactions between the PSA's and the steel surface (the G_0 in eq 1) may not be very strong with these formulations.

Figure 16 shows that shear resistance increased with the gel content. Shear resistance is related with the cohesive strength of the adhesive that increased with the gel content. Interestingly, latex 1 has a better shear resistance than latex 4, consistent with the differences in tensile behavior observed at low strain rates in Figure 13a. This difference suggests a different polymer architecture for the two latexes although it is not readily detectable by the gel content and swelling ratio measurements.

Conclusions

In the foregoing, the feasibility of independent control of the gel fraction and sol molecular weight distribution in the miniemulsion polymerization of 2-ethylhexyl acrylate using symmetrical (ethylene glycol dimethacrylate, EGDMA) and nonsymmetrical (allyl methacrylate, AMA) cross-linkers and a chain transfer agent (*n*-dodecyl mercaptan) was investigated. In addition, the effect of the polymer architecture on the adhesive properties was studied.

It was found that neither the polymerization rate nor the number of particles was affected by the presence of cross-linker and chain transfer agent. The highly reactive symmetrical cross-linker had almost no effect on gel content, swelling, and sol MWD, likely because extensive primary cyclization underwent by the highly reactive symmetrical cross-linker. Allyl methacrylate, a nonsymmetrical cross-linker with functional groups having very different reactivity, showed a strong effect on polymer architecture. Polymer characteristics were very sensitive to the chain transfer agent, and widely different polymers were obtained varying the concentration and feeding strategy of the CTA. Adhesion properties were mainly controlled by the gel content. Both tack and peel resistance showed a maximum for a relatively low gel content (15%), whereas shear resistance continuously increased with gel.

Acknowledgment. The authors thank the financial support provided by Diputación Foral de Gipuzkoa, Eusko Jaurlaritza (GIC07/16-II-303-07), and the Ministerio de Educación y Ciencia (MEC CTQ 2006-03412).

References and Notes

(1) Toyama, M.; Ito, T.; Nukatsuka, H. *J. Appl. Polym. Sci.* **1973**, *17*, 3495–3502.
(2) Satas, D. *Handbook of Pressure Sensitive Adhesives Technology*, 2nd ed.; Van Nostrand Reinhold: New York, 1989.
(3) Gilbert, F. X.; Allal, A.; Marin, G.; Derail, C. *J. Adhes. Sci. Technol.* **1999**, *13*, 1029–1044.
(4) Crosby, A. J.; Shull, K. R. *J. Polym. Sci., Polym. Phys.* **1999**, *37*, 3455–3472.
(5) Tobing, S. D.; Klein, A. *J. Appl. Polym. Sci.* **2000**, *76*, 1965–1976.
(6) Tobing, S. D.; Klein, A.; Sperling, L. H.; Petrasko, B. *J. Appl. Polym. Sci.* **2001**, *81*, 2109–2117.
(7) Tobing, S. D.; Klein, A. *J. Appl. Polym. Sci.* **2001**, *79*, 2230–2244.
(8) Jovanovic, R.; Dubé, M. A. *J. Macromol. Sci., Polym. Rev.* **2004**, *44*, 1–51.
(9) Jovanovic, R.; McKenna, T. F.; Dubé, M. A. *Macromol. Mater. Eng.* **2004**, *289*, 467–474.
(10) Park, M. C.; Lee, M. C. *J. Appl. Polym. Sci.* **2004**, *94*, 1456–1460.
(11) Shanks, R. A.; Gower, M. A. *Macromol. Chem. Phys.* **2005**, *206*, 1015–1027.
(12) do Amaral, M.; Roos, A.; Asua, J. M.; Creton, C. *J. Colloid Interface Sci.* **2005**, *281*, 325–338.
(13) Mallegol, J.; Bennett, G.; McDonald, P. J.; Keddie, J. L.; Dupont, O. *J. Adhes.* **2006**, *82*, 217–238.
(14) Plessis, C.; Arzamendi, G.; Leiza, J. R.; Schoonbrood, H. A.; Charmot, D.; Asua, J. M. *Macromolecules* **2000**, *33*, 5041–5047.
(15) Plessis, C.; Arzamendi, G.; Alberdi, J. M.; Agnely, M.; Leiza, J. R.; Asua, J. M. *Macromolecules* **2001**, *34*, 6138–6143.
(16) Plessis, C.; Arzamendi, G.; Leiza, J. R.; Alberdi, J. M.; Schoonbrood, H. A.; Charmot, D.; Asua, J. M. *J. Polym. Sci., Polym. Chem.* **2001**, *39*, 1106–1119.
(17) Chauvet, J.; Leiza, J. R.; Asua, J. M. *Polymer* **2005**, *46*, 9555–9561.
(18) Heatley, F.; Lovell, P. A.; Yamashita, T. *Macromolecules* **2001**, *34*, 7636–7641.
(19) Ugelstad, J.; El-Aasser., M. S.; Vanderhoff, J. W. *J. Polym. Sci., Polym. Lett.* **1973**, *11*, 503–513.
(20) Asua, J. M. *Prog. Polym. Sci.* **2002**, *27*, 1283–1346.
(21) Delgado, J.; El-Aasser, M. S.; Silebi, C. A.; Vanderhoff, J. W.; Guillot, J. *J. Polym. Sci., Polym. Phys.* **1988**, *26*, 1495–1517.
(22) Lakrout, H.; Sergot, P.; Creton, C. *J. Adhes.* **1999**, *69*, 307–356.
(23) Josse, G.; Sergot, P.; Creton, C.; Dorget, M. *J. Adhes.* **2004**, *80*, 87–118.
(24) American Society for Tapes and Materials, Norm ASTM: D1876-95, Standard test method for peel resistance of adhesives, 1996.
(25) American Pressure Sensitive Tape Council, Norm PSTC-7M. Holding Power of Pressure Sensitive Tapes, 1986.
(26) American Society of Materials, Norm ASTM: D3654/C3654M-02, Standard test tapes, 1999.

(27) Rodriguez, R.; Barandiaran, M. J.; Asua, J. M. *Polymer* **2008**, *49*, 691–696.
(28) Elliot, J. E.; Bowman, C. N. *Macromolecules* **1999**, *32*, 8621–8628.
(29) Anseth, J. W.; Elliot, J. E.; Bowman, C. N. *Chem. Eng. Sci.* **2001**, *56*, 3173–3184.
(30) Elliot, J. E.; Bowman, C. N. *Macromolecules* **2002**, *35*, 7125–7131.
(31) Bouvier-Fontes, L.; Pirri, R.; Asua, J. M.; Leiza, J. R. *Macromolecules* **2005**, *38*, 1164–1171.
(32) Deplace, F.; Carelli, C.; Mirot, S.; Retsos, H.; Chateauminois, A.; Ouzineb, K.; Creton, C. *J. Adhes.* **2009**, *85*, 18–54.
(33) Creton, C.; Lakrout, H. *J. Polym. Sci., Polym. Phys.* **2000**, *38*, 965–979.
(34) Creton, C. *MRS Bull.* **2003**, *28*, 434–439.